studies with the anticipated changes in the energy and water balances from AGCM investigations in order for a complete picture of the total environmental response to increased CO_2 to emerge.

In the tropics, it is projected that the value of A for the terrestrial biosphere is inversely related to changes in T under $2 \times CO_2$ conditions (see the RPV-RP axis in Fig. 4A). For the northern latitudes, this is true for the growing season but, because of the lower winter temperatures associated with the RPV case, the mean annual A and T values appear to be correlated (Fig. 4B). For the globe, the net result is that total A varies widely for little variation in the global mean value of T (Fig. 4C).

We performed these simulations using observed vegetation conditions for 1987, as obtained from satellite data. We did not consider morphological responses (that is, changes in leaf area index or greenness) or changes in vegetation type (migration of biomes) in response to altered climate or plant physiology. Human impacts on the distribution of vegetation are likely to be important but are difficult to predict. The potential effect of plant physiology on climate is simulated to be substantially larger when physiology is down-regulated than when it is not (PV versus P and RPV versus RP). However, there is a large uncertainty as to whether the aggregate terrestrial biospheric response will be closer to the unadjusted (RP) case or the down-regulated (RPV) case.

REFERENCES AND NOTES

1. J. T. Houghton, G. J. Jenkins, J. J. Ephraums, Eds., *Climate Change: The IFCC Scientific Assessment* (World Meteorological Organization–United Nations Environment Programme, Cambridge Univ. Press, Cambridge, 1990).
2. I. R. Cowan, *Adv. Bot. Res.* **4**, 117 (1977).
3. G. J. Collatz, J. T. Ball, C. Grivet, J. A. Berry, *Agric. For. Meteorol.* **54**, 107 (1991); G. J. Collatz, M. Ribas-Carbo, J. A. Berry, *Aust. J. Plant Physiol.* **19**, 519 (1992).
4. C. B. Field, F. S. Chapin III, P. A. Matson, H. A. Mooney, *Annu. Rev. Ecol. Syst.* **23**, 201 (1992); D. T. Tissue, R. B. Thomas, B. R. Strain, *Plant Cell Environ.* **16**, 859 (1993).
5. C. A. Gunderson and S. D. Wullschleger, *Photosynth. Res.* **39**, 369 (1994); C. B. Field, in *Response of Plants to Multiple Stresses*, H. A. Mooney, W. E. Winner, E. J. Pell, Eds. (Academic Press, San Diego, CA, 1991), pp. 35–65.
6. C. B. Field, R. B. Jackson, H. A. Mooney, *Plant Cell Environ.* **18**, 1214 (1995).
7. J. I. L. Morison, in *Stomatal Function*, E. Zeiger, G. D. Farquhar, I. R. Cowan, Eds. (Stanford Univ. Press, Stanford, CA, 1987), pp. 229–252.
8. D. J. Beerling and W. G. Chaloner, *Rev. Palaeobot. Palynol.* **81**, 11 (1994); J. Penuelas and R. Matamala, *J. Exp. Bot.* **41**, 1119 (1990); F. I. Woodward, *Nature* **327**, 617 (1987).
9. P. J. Sellers, J. A. Berry, G. J. Collatz, C. B. Field, F. G. Hall, *Remote Sensing Environ.* **42**, 187 (1992).
10. P. J. Sellers *et al.*, *J. Climate*, in press.
11. D. A. Randall *et al.*, *ibid.*, in press.
12. T. G. Jensen, *Department of Atmospheric Science Paper 593*, Colorado State University (1995).
13. P. J. Sellers *et al.*, *J. Climate*, in press.
14. J. L. Dorman and P. J. Sellers, *J. Appl. Meteorol.* **28**, 833 (1989).
15. P. J. Sellers, M. D. Heiser, F. G. Hall, *J. Geophys. Res.* **97**, 19033 (1992); P. J. Sellers *et al.*, *ibid.* **100**, 25607 (1995).
16. P. Ciais, P. P. Tans, M. Trolier, J. W. C. White, R. J. Francey, *Science* **269**, 1098 (1995); A. S. Denning, I. Fung, D. A. Randall, *Nature* **376**, 240 (1995); P. Ciais *et al.*, *J. Geophys. Res.* **100**, 5051 (1995).
17. J. Hansen *et al.*, *Climate Process and Climate Sensitivity*, J. E. Hansen and T. Takahashi, Eds. (Maurice Ewing Series 5, American Geophysical Union, Washington, DC, 1984), pp. 130–163.
18. Our results are at odds with those reported in two previous studies (*19*, *20*). The land surface parameterizations used in those two studies were based on highly empirical leaf stomatal conductance formulations that were not linked to photosynthetic processes. Also, the location and state of the global vegetation were based on extrapolations from a relatively small number of ground surveys reported in the ecological literature. Both studies imposed a halving (that is, a 50% reduction) of stomatal conductance everywhere, which may be compared with the reductions of between 25% (P and RP cases) and 35% (PV and RPV cases) calculated for g_c in our study. In one of the studies (*19*), evapotranspiration in the tropics was almost unaffected by physiological effects; this may be because that model distributes convective precipitation evenly over land grid squares, resulting in an overestimation of canopy interception loss and a reduction in the importance of canopy transpiration to the total latent heat flux. Both studies projected significant impacts of physiological effects in the boreal zone in July, which led to increases in surface temperature there. For the same area, our results indicate that the combined (radiative plus physiological) responses to $2 \times CO_2$ yield only a slight warming relative to the R case in summer and a slight cooling in winter (Fig. 3).
19. A. Henderson-Sellers, K. McGuffie, C. Gross, *J. Climate* **8**, 1738 (1995).
20. D. Pollard and S. L. Thompson, *Global Planet. Change* **10**, 1229 (1995).
21. C. A. Nobre, P. J. Sellers, J. Shukla, *J. Climate* **4**, 957 (1991).

22. Supported by NASA Earth Observing System (EOS) funds (Sellers-Mooney Interdisciplinary Science Project). We gratefully acknowledge encouragement and support from G. Asrar and thank the NASA Center for Computational Sciences for their cooperation and L. Blasingame and V. McElroy for typing the manuscript.

17 October 1995; accepted 16 January 1996

The Amyloid Precursor Protein of Alzheimer's Disease in the Reduction of Copper(II) to Copper(I)

Gerd Multhaup,* Andrea Schlicksupp, Lars Hesse, Dirk Beher, Thomas Ruppert, Colin L. Masters, Konrad Beyreuther

The transition metal ion copper(II) has a critical role in chronic neurologic diseases. The amyloid precursor protein (APP) of Alzheimer's disease or a synthetic peptide representing its copper-binding site reduced bound copper(II) to copper(I). This copper ion–mediated redox reaction led to disulfide bond formation in APP, which indicated that free sulfhydryl groups of APP were involved. Neither superoxide nor hydrogen peroxide had an effect on the kinetics of copper(II) reduction. The reduction of copper(II) to copper(I) by APP involves an electron-transfer reaction and could enhance the production of hydroxyl radicals, which could then attack nearby sites. Thus, copper-mediated toxicity may contribute to neurodegeneration in Alzheimer's disease.

The major component of Alzheimer's disease (AD) amyloid βA4 is derived from the transmembrane protein APP (*1*). The central role of APP has emerged from the identification of genes that cosegregate with the disease and influence βA4 formation (*2*). The normal cellular function of APP is unknown. Work with different cell lines has shown that the secreted or membrane-associated forms of APP regulate cell growth and neurite length and participate in cell-cell and cell-matrix adhesion (*3*). APP binds to collagen, laminin, and heparan sulfate side chains of proteoglycans (*4*). APP isoforms (containing the Kunitz protease inhibitor domain) that form complexes with extracellular proteases are internalized by the apolipoprotein E receptor LRP (low density lipoprotein receptor–related protein) (*5*). A Zn(II)-binding site resides within APP residues 181 to 200 (*6*), and a Cu(II)-binding site resides within APP residues 135 to 155 (*6*, *7*). Zn(II) and Cu(II) binding influence APP conformation, stability, and homophilic interactions (*6*, *7*). In the *APP* gene family, both binding sites are conserved in *APLP2*, whereas in *APLP1* only the Zn(II) site is present (*6*, *7*).

In neurons, APP is first delivered from the cell body to the axonal cell surface and then to the dendritic plasma membrane (*8*). If APP undergoes transcytosis from axons to dendrites, APP could function as a transcytotic receptor in neurons and could facilitate the transcellular transport of cerebral Zn(II) and Cu(II). Copper is an important component of various redox enzymes. Free Cu is also a toxic ion, as exemplified by its ability to inactivate proteins through ty-

G. Multhaup, A. Schlicksupp, L. Hesse, D. Beher, K. Beyreuther, ZMBH–Center for Molecular Biology Heidelberg, University of Heidelberg, Im Neuenheimer Feld 282, D-69120 Heidelberg, Germany.
T. Ruppert, Department of Virology, University of Heidelberg, D-69120 Heidelberg, Germany.
C. L. Masters, Department of Pathology, University of Melbourne, Parkville, Victoria 3052, Australia, and Neuropathology Laboratory, Mental Health Research Institute of Victoria, Parkville, Victoria 3052, Australia.

*To whom correspondence should be addressed. E-mail: gmulthaup@sun0.urz.uni-heidelberg.de

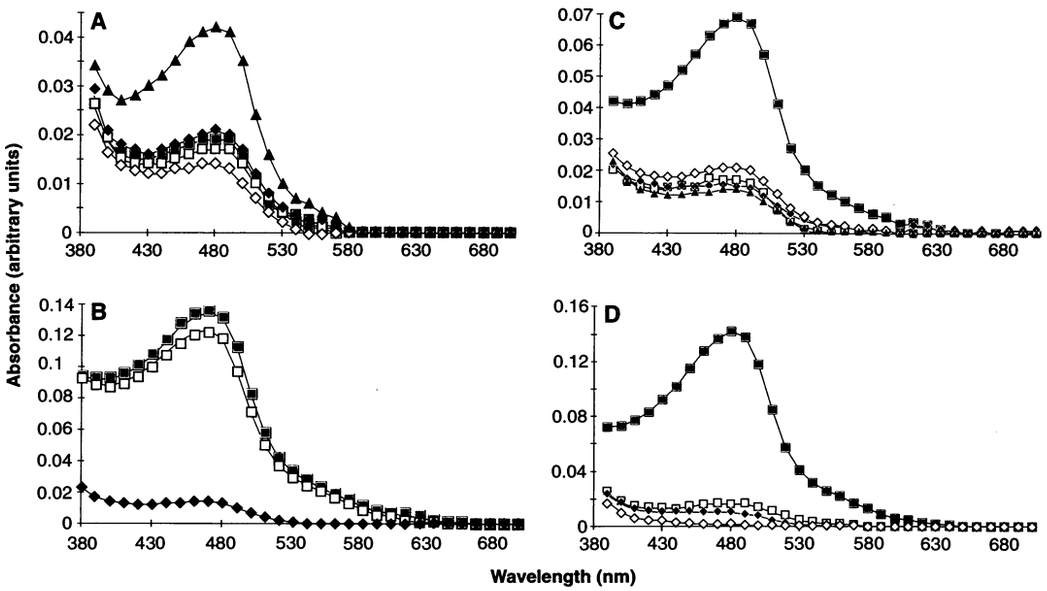

Fig. 1. (**A**) Reduction of Cu(II) to Cu(I) by APP. The production of Cu(I) was quantitated by recording the complex formation of Cu(I) with BC, as described (*25*). Wavelength scans from 380 to 700 nm revealed an absorbance maximum of the Cu(I)-BC complex at 480 nm. The spectra of samples containing the Cu(I) indicator molecule BC (360 μM), APP (12 μg/ml), and Cu(II) (10 μM) in phosphate-buffered saline (PBS) are shown after incubation at 37°C for 60 min. Incubations contained BC and Cu(II) (◇); BC, Cu(II), and KLH (12 μg/ml) (□); BC, Cu(II), and SOD (12 μg/ml) (■); BC, Cu(II), and ovalbumin (12 μg/ml) (◆); or BC, Cu(II), and hs-APP (12 μg/ml) (▲). For each incubation, a single spectrum representative of two independent experiments is shown; hs-APP was purified as described (*5*, *7*). Chemicals used in all experiments are described in (*26*). (**B**) Reduction of Cu(II) to Cu(I) by TP-APP_{770} and TP-APP_{N262}. Absorbance spectra of samples containing combinations of BC, TP-APP_{770} (20 μg/ml), TP-APP_{N262} (20 μg/ml), and Cu(II) were recorded as described in (A). After carboxymethylation, TP-APP_{770} and TP-APP_{N262} failed to reduce Cu(II) to Cu(I). Incubations contained BC, Cu(II), and carboxymethylated TP-APP_{N262} (◆); BC, Cu(II), and TP-APP_{N262} (□); or BC, Cu(II), and TP-APP_{770} (■). For each incubation, a single spectrum representative of three independent experiments is shown. Carboxymethylation was performed as described (*27*). (**C**) Reduction of Cu(II) to Cu(I) by $APP_{135-156}$. A synthetic peptide corresponding to APP residues 135 to 156 was able to reduce Cu(II) to Cu(I). Absorbance spectra of samples containing combinations of BC, $APP_{135-156}$ (5 μg/ml), control peptides (5 μg/ml), and Cu(II) are shown. Incubations contained BC and Cu(II) (▲) or BC, Cu(II), and the synthetic peptides representing APP residues 435 to 456 (◆), 327 to 348 (□), 303 to 324 (◇), or 135 to 156 (■). $APP_{135-156}$ was identified to bind Cu(II) (*7*); other peptides were used as controls. All failed to show Cu(II) binding in LC-ESI MS analysis. Peptides were synthesized by solid-phase fluorenyl methoxy carbonyl chemistry. (**D**) Dependence of reduction of Cu(II) to Cu(I) on a free sulfhydryl group in $APP_{135-156}$. Absorbance spectra of samples containing combinations of BC (360 μM), $APP_{135-156}$ (40 μg/ml), $APP_{135-156}$ (40 μg/ml) pretreated with *N*-ethylmaleimide (10 mM for 30 min), and Cu(II) are shown. Incubations contained BC and $APP_{135-156}$ pretreated with *N*-ethylmaleimide (◇); BC and Cu(II) (◆); BC, Cu(II), and $APP_{135-156}$ pretreated with *N*-ethylmaleimide (□); or BC, Cu(II), and $APP_{135-156}$ (■).

rosine nitration, and both deficiency and excess lead to disorders such as Wilson's disease, Menkes' syndrome, and possibly familial amyotrophic lateral sclerosis (FALS) (*9*–*12*). The candidate genes for these diseases encode membrane proteins that are homologous to bacterial membrane Cu(II) and Cd(II) transporters and Cu-Zn superoxide dismutase (SOD) (*13*). Because transmembrane APP binds Cu(II), our working hypothesis was that APP is involved in Cu homeostasis and that accumulation of APP in neurites, such as occurs in AD (*11*, *14*), may lead to disruption of Cu compartmentalization and hence to Cu toxicity.

We incubated human APP (hs-APP; 12 μg/ml), bacterial fusion proteins of APP (TP-APP_{770} and TP-APP_{N262}; 12 μg/ml), and a synthetic peptide that represents the Cu-binding site of APP ($APP_{135-156}$) with physiological concentrations of Cu(II) (10 μM) at 37°C for 60 min in the presence of the Cu(I) indicator molecule bathocuproine disulfonate (BC; 360 μM). Incubation of Cu(II) with APP resulted in reduction to Cu(I), as indicated by the formation of a peak with maximal absorbance at 480 nm, which is characteristic of the BC-Cu(I) complex (Fig. 1A). In contrast, after incubation of other Cu(II)-binding proteins such as SOD, keyhole limpet hemocyanin (KLH), or ovalbumin (12 μg/ml of each) with Cu(II) for 60 min, no increase in absorbance at 480 nm was observed (Fig. 1A). The wavelength scans for the interaction of TP-APP_{770} and TP-APP_{N262} showed the same reduction of Cu(II) to Cu(I) (Fig. 1B). Carboxymethylation of TP-APP_{770} prevented Cu(I) formation, which suggested that the oxidation of cysteines was necessary for the reduction of Cu(II) (Fig. 1B). Thus, the NH_2-terminal 262 residues of APP are sufficient for this catalytic activity. To localize further the active site responsible for the redox reaction, we tested a peptide corresponding to APP residues 135 to 156 ($APP_{135-156}$). This peptide was able to reduce Cu(II) to Cu(I) (Fig. 1C). Preincubation of $APP_{135-156}$ with *N*-ethylmaleimide abolished the reduction of Cu(II), which indicated that the free sulfhydryl group of $APP_{135-156}$ was involved (Fig. 1D).

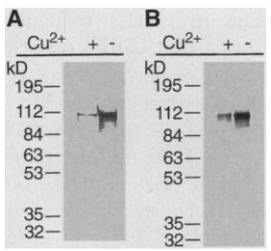

Fig. 2. Copper-dependent oxidative modification of TP-APP_{770}. During the incubation of TP-APP_{770} with Cu(II) (Fig. 1A) and the following redox reaction, formation of APP dimers was not observed, as assessed by electrophoretic mobility of APP on SDS gels. TP-APP_{770} (20 μg/ml) was incubated in PBS at 37°C for 1 hour without (−) or with (+) Cu(II) (10 μM). Electrophoretic mobility was measured in the presence (**A**) or absence (**B**) of mercaptoethanol. Copper-treated TP-APP_{770} (0.6 μg) was precipitated (*24*) and untreated protein (0.6 μg) was loaded directly, separated on an 8% polyacrylamide gel, and stained with silver (*28*). This finding also implies that disulfide bonds did not occur randomly in the recombinant TP-APP_{770} (*29*).

To differentiate between inter- and intramolecular formation of disulfide bonds, we examined an aliquot of Cu(II)-oxidized TP-APP_{770} for dimer formation with SDS–polyacrylamide gel electrophoresis (SDS-PAGE) under nonreducing and reducing conditions (Fig. 2). APP dimer formation, which may result in the formation of intramolecular disulfide bonds during the production of the cuprous ions by TP-APP_{770}, was not observed. Thus, in full-length APP the second cysteine required for the redox reaction would be from within the same molecule.

Having identified a Cu(II)-binding site in APP and ascertained that APP had an intrinsic redox potential specific for Cu(II), we next investigated the involvement of cys-

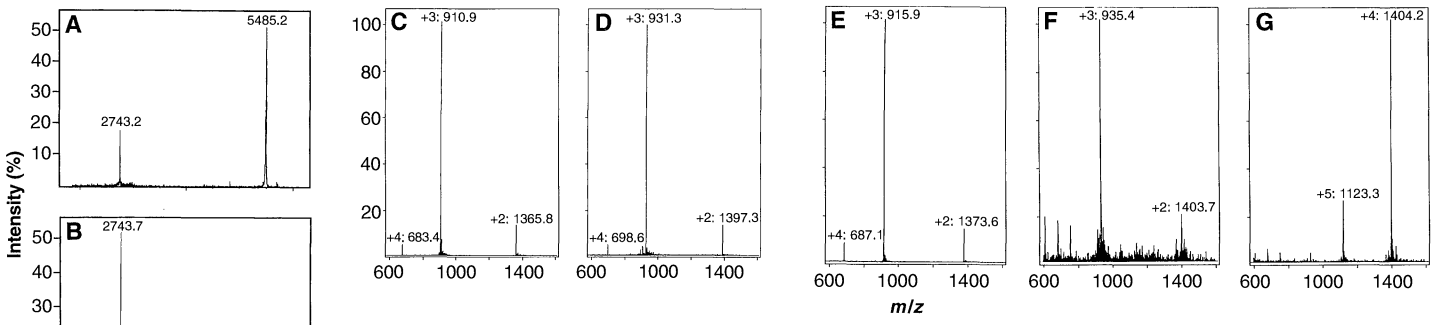

Fig. 3. Determined mass of the Cu-oxidized synthetic peptide $APP_{135-156}$ by MALDI and LC-ESI MS analysis. (**A**) The MALDI MS spectrum is shown for $APP_{135-156}$ after Cu(II) treatment, as described in Fig. 1C. The molecular mass of 2743.2 corresponds to the native peptide; the molecular mass of 5485.2 corresponds to the disulfide-linked dimer. Methods were as described (*30*). (**B**) Under the same conditions for incubation as in (A) with Zn(II), Ni(II), Co(II), and Mg(II), almost no doubly charged masses were observed. The molecular mass of 2743.7 corresponds to the monomeric form of the native peptide. (**C**) Illustrative spectra of LC-ESI MS analysis (*29*) for a control sample without Cu(II) pretreatment. The charge states (+2) to (+5) are shown, followed by the *m/z* value. (**D**) The full-scan spectrum, showing a mutant peptide of $APP_{135-156}$ with a serine instead of cysteine with one bound Cu. (**E**) ESI spectra showing the dramatic difference in intensity and *m/z* values for $APP_{135-156}$ before addition of Cu(II). (**F**) After addition of Cu(II), the stoichiometry of Cu(II) binding is 1:1 for the monomer, and (**G**) consequently, 2:1 for the $APP_{135-156}$ dimer. For methods see (*29*).

teines (*6*, *7*). The candidate region in APP for Cu(II) binding (residues 135 to 155) contains a single cysteine at position 144 that may represent one of the cysteines in the active site. Preliminary studies with surface plasmon resonance analysis indicated a structural change of APP initiated by Cu(II) (*7*). Because Cu(II) was reduced to Cu(I) by APP, this conformational change may have resulted from cystine formation involving Cys^{144}. Thus, we used matrix-assisted laser desorption mass spectrometry to analyze directly the possible participation of this cysteine in Cu(II) reduction. This analysis showed that Cu(II) specifically induced oxidation of the single cysteine residue contained within peptide $APP_{135-155}$. The incubation of the peptide with Cu(II) [synthetic peptide (200 μg/ml); 1 mM divalent ions], but not with Zn(II), Ni(II), Co(II), or Mg(II), led to dimerization of peptides containing Cys^{144} (Fig. 3, A and B). In contrast to full-length APP (Fig. 2), which did not dimerize during the reaction, $APP_{135-156}$ peptides formed intermolecular disulfide bridges, most likely because of the lack of a second intramolecular cysteine. Electrospray mass spectrometry also revealed that a peptide with a serine replacement at position 144 still bound Cu(II) but did not have the catalytic activity (Fig. 3, C and D).

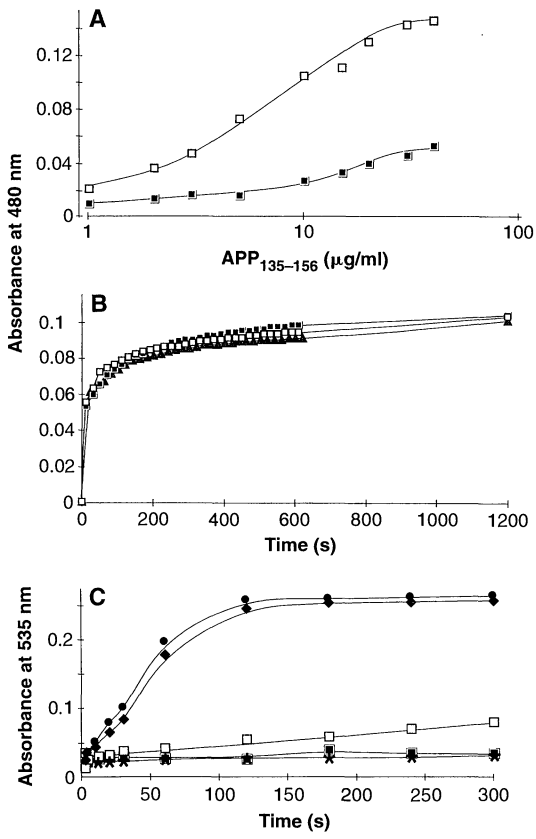

Fig. 4. (**A**) Dependence of Cu(II) reduction on concentration of $APP_{135-156}$. $APP_{135-156}$ was incubated in PBS at 37°C for 60 min with Cu(II) (10 μM) and BC (360 μM), without (□) and with GHL (5 μg/ml) (■). Cu(I) formation was monitored as the increase in absorbance at 480 nm. Each point represents the mean of at least two independent experiments. (**B**) Effects of SOD and catalase on Cu(II) reduction by $APP_{135-156}$. Cu(II) (10 μM) and $APP_{135-156}$ (20 μg/ml) were incubated in PBS at 37°C for 60 min with BC (360 μM) in the absence (■) or presence of either SOD (1000 U/ml, □) or catalase (1000 U/ml, ▲). Cu(I) formation was monitored as the increase in absorbance at 480 nm. (**C**) Lack of Fe(III) reduction by APP. Absorbance at 535 nm was measured for various combinations of BP (360 μM), hs-APP (12 μg/ml), $APP_{135-156}$ (20 μg/ml), and Fe(III)-citrate (10 μM) in PBS and is shown after incubation at 37°C for 60 min. Incubations contained BP, Fe(III)-citrate, and hs-APP (*); BP and Fe(III)-citrate (■); BP, Fe(III)-citrate, and $APP_{135-156}$ (□); BP, Fe(III)-citrate, $APP_{135-156}$, and the hypoxanthine (1.5 mM)–xanthine oxidase (0.02 U/ml) MFO system (◆); or BP, Fe(III)-citrate, hs-APP, and the hypoxanthine (7.3 mM)–xanthine oxidase (0.2 U/ml) MFO system (●). Fe(II) formation was monitored as the increase in absorbance at 535 nm. Each point represents the mean of at least two independent experiments. Fe(II) was quantitated according to (*16*).

Preformed $APP_{135-156}$ dimers had Cu ion–binding properties similar to those of the monomeric peptide. The stoichiometry of Cu(II) binding was 1:1 for the monomer (Fig. 3, E and F) and 2:1 for the dimer of $APP_{135-156}$ (Fig. 3G). Thus, the Cu-binding site remained intact after dimer formation, and formation of one intermolecular disulfide bridge did not interfere with Cu binding. Also, Cu-coordinating histidines (*7*) remained available in the dimers for interaction with Cu ions. Analyses of Cu(II) reduction by $APP_{135-156}$ and variants thereof corroborated these findings. Peptides that did not contain Cys^{144} (*7*) failed to show a reduction of Cu(II), and rates of Cu(I)-BC complex formation were at the background level. Peptides that carried amino acid substitutions at histidines (*7*) but contained Cys^{144} showed a diminished potential for Cu(II) reduction that varied depending on the position of the altered residue. The variant peptide N3 (*7*) reached only 30% of the redox activity of wild-type $APP_{135-156}$. The His substitution N13 showed a slightly reduced redox activity of 78% compared with that of $APP_{135-156}$. Thus, more than one histidine residue was required for binding and subsequent reduction of Cu(II). The corresponding peptide of APLP2 (*7*), the most closely related member within the APP superfamily, had 60% of the activity of $APP_{135-156}$. This difference implies an influence of residues that are not conserved between APP and

APLP2 for Cu(II) binding and reduction.

To investigate the dependence of $APP_{135-156}$ concentration on Cu(II) reduction, we incubated 10 μM Cu(II) for 60 min at 37°C with BC (360 μM) in the presence of increasing concentrations of $APP_{135-156}$ (0 to 80 μg/ml). Maximal amounts of Cu(I) (about 7.5 μM) were observed at $APP_{135-156}$ concentrations of 10 μM (25 μg of peptide per milliliter) (Fig. 3A). Below this concentration, $APP_{135-156}$ reduced Cu(II) in a dose-dependent manner. Cu(I)-BC complex formation was observed at 0.4 μM (1.0 μg of peptide per milliliter) (Fig. 4A). The human plasma copper-binding growth factor glycyl-L-histidyl-L-lysine (GHL) (*15*) was a potent inhibitor of $APP_{135-156}$ oxidation by Cu(II). At concentrations as low as 5 μg of GHL per milliliter, a 70% inhibition of $APP_{135-156}$ activity was observed, independent of the $APP_{135-156}$ concentration used (Fig. 4A). GHL presumably acts by converting GHL into GHL-Cu, thus chelating ionic copper and preventing its binding to $APP_{135-156}$. The reduction of Cu(II) by $APP_{135-156}$ was not inhibited by SOD or by catalase (Fig. 4B). Thus, the redox reaction did not require superoxide and hydrogen peroxide.

In contrast to the ability of APP to reduce Cu(II) to Cu(I), APP did not reduce Fe(III) to Fe(II) (Fig. 4C). The latter was analyzed as complex formation of Fe(II) with the indicator molecule bathophenanthroline disulfonate (BP). Even after 5 hours of incubation, a BP-Fe(II) complex was not formed when hs-APP was incubated either with Fe(III)-citrate (10 μM) and BP (360 μM) or with peptide $APP_{135-156}$. However, when a standard mixed-function oxidase system [MFO; 1.5 mM hypoxanthine with xanthine oxidase (0.19 U/ml)] was added as a source of superoxide (*16*), Fe(III) was reduced rapidly to Fe(II), independently of the presence of hs-APP or $APP_{135-156}$ (Fig. 4C).

Thus, Cu(II) binding led to oxidative modification of APP, giving rise to cystine and Cu(I) formation. Accordingly, in vitro APP has a function in electron transfer to Cu(II). Once Cu(I) is formed, in the presence of peroxides it may produce activated oxygen species ($\cdot OH$, O_2^-). The Cu(II)-reducing activity of APP may occur on or near the cell surface because the redox state of cytosol in viable cells is reducing in the absence of exogenous reductant (*17*). APP-Cu(I) complexes on the surface of neurons may be particularly vulnerable to peroxides generated by extracellular SOD and by various mechanisms including activated microglia.

In Down syndrome a gene dosage effect involving Cu-Zn SOD and APP may be responsible for premature onset of AD (*18*). Copper homeostasis could be adversely affected in an interplay of APP and SOD, as has been suggested for a similar mechanism of Cu toxicity with mutant SOD in FALS (*13*). Copper reaches concentrations in body fluids of about 10 μM and has been discussed as a possible effector of βA4 aggregation in AD (*19, 20*). Also, in cerebrospinal fluid of AD patients, concentrations of Cu were as much as 2.20 times the concentrations in control groups (*19, 21*). Two major hypotheses have been proposed concerning the mechanism of amyloid deposition in AD (*11, 14*). In one hypothesis, synaptic and axonal injury leading to the formation of dystrophic neurites with accumulations of APP may precede the deposition of βA4 (*14*). The alternative view is that amorphous βA4 deposits (diffuse plaques) constitute the first abnormality (*18*). A mechanism of disease mediated by disruption of vesicular-mediated APP-Cu(I) complex trafficking is consistent with both hypotheses. In the presence of hydrogen peroxide, the key feature of such an APP-Cu(I) accumulation would be the gain of Cu-mediated toxicity. The final common pathway in AD may be oxygen radical–induced cellular damage and radical-mediated aggregation of βA4 monomers, which produce toxic forms of βA4 (*22*).

REFERENCES AND NOTES

1. K. Beyreuther *et al.*, *Ann. N.Y. Acad. Sci.* **695**, 91 (1993); D. J. Selkoe, *Annu. Rev. Neurosci.* **17**, 489 (1994).
2. E. Levy *et al.*, *Science* **248**, 1124 (1990); E. Levy-Lahad *et al.*, *ibid.* **269**, 973 (1995); E. H. Corder *et al.*, *ibid.* **261**, 921 (1993); N. Suzuki *et al.*, *ibid.* **264**, 1336 (1994); J. Murrell, M. Farlow, B. Ghetti, M. D. Benson, *ibid.* **254**, 97 (1991); X.-D. Cai, T. E. Golde, S. G. Younkin, *ibid.* **259**, 514 (1993); A. Goate *et al.*, *Nature* **349**, 704 (1991); M.-C. Chartier-Harlin *et al.*, *ibid.* **353**, 844 (1991); R. Sherrington *et al.*, *ibid.* **375**, 754 (1995); C. Haass *et al.*, *ibid.* **359**, 322 (1992); L. Hendriks *et al.*, *Nature Genet.* **1**, 218 (1992); M. Mullan *et al.*, *ibid.*, p. 345; B. T. Hyman *et al.*, *Proc. Natl. Acad. Sci. U.S.A.* **92**, 3586 (1995).
3. B. D. Shivers *et al.*, *EMBO J.* **7**, 1365 (1988); T. Saitoh *et al.*, *Cell* **58**, 615 (1989); J. M. Roch *et al.*, *J. Biol. Chem.* **267**, 2214 (1992); E. A. Milward *et al.*, *Neuron* **9**, 129 (1992).
4. K. C. Breen, M. Bruce, B. H. Anderton, *J. Neurosci. Res.* **28**, 90 (1991); G. Multhaup, A. I. Bush, P. Pollwein, C. L. Masters, *FEBS Lett.* **355**, 151 (1994); S. Narindrasorasak *et al.*, *Lab. Invest.* **67**, 643 (1992); D. H. Small *et al.*, *J. Neurosci.* **14**, 2117 (1994).
5. M. Z. Kounnas *et al.*, *Cell* **82**, 331 (1995).
6. A. I. Bush *et al.*, *J. Biol. Chem.* **268**, 16109 (1993).
7. L. Hesse, D. Beher, C. L. Masters, G. Multhaup, *FEBS Lett.* **349**, 109 (1994).
8. T. Yamazaki, D. J. Selkoe, E. H. Koo, *J. Cell Biol.* **129**, 431 (1995); M. Simons *et al.*, *J. Neurosci. Res.* **41**, 121 (1995).
9. R. E. Tanzi *et al.*, *Nature Genet.* **5**, 344 (1993); P. C. Bull, G. R. Thomas, J. M. Rommens, J. R. Forbes, D. W. Cox, *ibid.*, p. 327; C. Vulpe, B. Levinson, S. Whitney, S. Packman, J. Gitschier, *ibid.* **3**, 7 (1993); Y. Yamaguchi, M. E. Heiny, J. D. Gitlin, *Biochem. Biophys. Res. Commun.* **197**, 271 (1993).
10. J. Chelly *et al.*, *Nature Genet.* **3**, 14 (1993).
11. D. Wang and D. G. Munoz, *J. Neuropathol. Exp. Neurol.* **54**, 548 (1995).
12. J. S. Beckman, M. Carson, C. D. Smith, W. H. Koppenol, *Nature* **364**, 584 (1993); H. A. Hartmann and M. A. Evenson, *Med. Hypotheses* **38**, 75 (1992).
13. A. Odermatt, H. Suter, R. Krapf, M. Solioz, *J. Biol. Chem.* **268**, 12775 (1993); G. Nucifora, L. Chu, T. K. Misra, S. Silver, *Proc. Natl. Acad. Sci. U.S.A.* **86**, 3544 (1989); P. C. Wong *et al.*, *Neuron* **14**, 1105 (1995).
14. G. Giaccone *et al.*, *Neurosci. Lett.* **97**, 232 (1989); L. C. Cork, C. Masters, K. Beyreuther, D. L. Price, *Am. J. Pathol.* **137**, 1383 (1990).
15. L. Pickard and S. Lovejoy, *Methods Enzymol.* **147**, 314 (1987).
16. S. M. Lynch and B. Frei, *J. Lipid Res.* **34**, 1745 (1993).
17. H. F. Gilbert, *J. Biol. Chem.* **257**, 12086 (1982).
18. B. Rumble *et al.*, *N. Engl. J. Med.* **320**, 1446 (1989); C. J. Epstein *et al.*, *Proc. Natl. Acad. Sci. U.S.A.* **84**, 8044 (1987).
19. D. J. Fitzgerald, *Science* **268**, 1920 (1995).
20. C. O. Hershey *et al.*, *Neurology* **33**, 1350 (1983).
21. H. Basun, L. G. Forssel, L. Wetterberg, B. Winblad, *J. Neural Transm. Parkinson's Dis. Dementia Sect.* **3**, 231 (1991).
22. C. J. Pike and C. W. Cotman, *Neuroscience* **56**, 269 (1993); T. Dyrks, E. Dyrks, C. L. Masters, K. Beyreuther, *FEBS Lett.* **324**, 231 (1993).
23. M. Joselow and C. R. Dawson, *J. Biol. Chem.* **191**, 11 (1951); J. W. Landers and B. Zak, *Am. J. Clin. Pathol.* **29**, 590 (1958).
24. D. Wessel and U. I. Flügge, *Anal. Biochem.* **138**, 141 (1984).
25. Cu(I) and Fe(II) were quantitated with BC and BP, respectively. These indicator molecules specifically bind the reduced [Cu(I) and Fe(II)] but not the oxidized [Cu(II) and Fe(III)] forms of copper and iron (*23*). The Cu(I)-BC and Fe(II)-BP complexes thus formed exhibited absorbance maxima at 480 and 535 nm, respectively (see Figs. 1 and 4), permitting specific quantitation of Cu(I) and Fe(II).
26. Chemicals were purchased from Sigma (SOD, S-2515; catalase, C-40; BP, B-1375; hypoxanthine, H-9377; low density lipoprotein, L-5402; ovalbumin, A-5503; KLH, H-1757; and GHL, G-1887), Aldrich (BC, 14.662-59), Fluka (ferric citrate, 44941), or Serva (*N*-ethylmaleimide, 11331).
27. W. Landgraf, S. Regulla, H. E. Meyer, F. Hofmann, *J. Biol. Chem.* **266**, 16305 (1991).
28. C. R. Merril, D. Goldman, S. A. Sedman, M. H. Ebert, *Science* **211**, 1437 (1981).
29. H. S. Lu *et al.*, *J. Biol. Chem.* **267**, 8770 (1992).
30. Matrix-assisted laser desorption (MALDI) mass spectrometry (MS) was used to analyze dimerization of synthetic peptides. Analysis was performed on a Kratos KOMPACT MALDI III/TOF spectrometer (Kratos analytical) operating at an accelerating potential of 20 kV in the positive ion linear mode. Mass spectra were generated from the sum of 20 to 100 laser shots. External mass assignments were made with bovine insulin [mass-to-charge ratio (*m/z*) 5733.6] (Sigma, I-5500). In a typical experiment, 1 μl of a peptide sample (100 μg/ml) was mixed with 1 μl of matrix solution consisting of sinapinic acid (50 mM in 50% aqueous isopropanol). A 1-μl aliquot of this solution was placed on the probe tip and allowed to dry. LC electrospray MS (LC-ESI MS) was used to analyze Cu(II) binding of synthetic peptides modified according to published methods (*24*). Aliquots of 50 μl [10 mM ammonium acetate (pH 6.5), synthetic peptide (20 μg/ml), and 200 μM $CuCl_2$] were separated by reversed-phase high-performance liquid chromatography (SMART-system, equipped with a micro–reversed-phase chromatography C2/C18 SC 2.1/10 column; Pharmacia). Solvent A contained 10 mM ammonium acetate (pH 6.5); solvent B contained 10 mM ammonium acetate (pH 6.5) in 50% acetonitrile. Peptides were separated in a linear gradient running from 50% B to 100% B over 22 min. On-line analysis was performed with a tandem quadrupole mass spectrometer (TSQ7000; Finnigan-MAT, Bremen) equipped with an electrospray ion source. Each scan was acquired over the *m/z* range 600 to 1600 in 2 s. The peptides were identified by their molecular mass calculated from the *m/z* peaks of the single- or multiple-charged ions.

31. Supported by the Deutsche Forschungsgemeinschaft through Sonderforschungsbereich 317 (SFB317, A/11), the Bundesminister für Forschung and Technologie, and the Fonds der Chemischen Industrie. C.L.M. is supported by the National Health and Medical Research Council (Australia).

19 October 1995; accepted 22 December 1995